34th Annual International Conference of the IEEE EMBS
San Diego, California USA, 28 August - 1 September, 2012

Design Challenges for Camera Oximetry on a Mobile Phone

Walter Karlen[1,2], Joanne Lim[2], J. Mark Ansermino[2], Guy Dumont[2], and Cornie Scheffer[1]

Abstract— **The use of mobile consumer devices as medical diagnostic tools allows standard medical tests to be performed anywhere. Cameras embedded in consumer devices have previously been used as pulse oximetry sensors. However, technical limitations and implementation challenges have not been described. This manuscript provides a critical analysis of pulse oximeter technology and technical limitations of cameras that can potentially impact implementation of pulse oximetry in mobile phones. Theoretical and practical examples illustrate difficulties and recommendations to overcome these challenges.**

I. Introduction

Pulse oximetry (PO) provides a non-invasive measurement of the photoplethysmogram (PPG) which allows the extraction of heart rate (HR) and oxygen saturation (SpO_2). Since their introduction in the early 1980s, PO devices are widely used for continuous monitoring in critical care settings. PO can also be a powerful tool for spot checks, where an instant reading of vital signs can give the care provider a good overview of the state of the patient. To increase the mobility and affordability of PO devices, PO modules have been connected to mobile devices such as smartphones [1]. Mobile devices offer inherent resources, such as large screens, touch screen interfaces, up to quad-core processing power, high density batteries, and a wide range of networking solutions, that allow for the design of PO devices. Manufacturing costs are reduced by removing redundant hardware. Difficulties with distribution are eliminated as the innovation is provided only through software channels. As a result, the mobile phone can become a standalone medical device that provides point-of-care diagnostics anywhere. Reducing the frequency of patient transport and early monitoring can lessen the burden on health care systems and reduce costs. The technology will be available to anyone with a mobile phone, which is an essential requirement for true personalized medicine.

The integration of PO with mobile phones has recently progressed. A standard PO probe has been connected directly to the audio module that provides power and analog signal processing [2]. Another predominant sensor on mobile phones is the camera, which has been successfully used for assessment of HR in many software applications that are available in various software repositories and has also been explored by several research groups [3], [4], [5]. The principle of using an integrated camera for PPG recording is very elegant: the finger is directly placed onto the camera lens and illuminated with the LED flashlight. The intensity variation of the recorded video is processed and analyzed for heart beats. No external hardware is required by using the built-in camera. Another suggested approach is using an external camera device (e.g. webcam) that requires no skin contact. The color changes of the skin are recorded by the camera, either with additional lighting [6], [7] or without [8], [9]. Similar to the integrated camera approach, the recorded video frames are compared to detect variation in intensity that is attributed to changes in blood volume.

The question that remains is whether consumer grade cameras on mobile phones can provide an accurate measurement of SpO_2. PO devices are required to comply with ISO standards [10] and a high accuracy of $< 4\% \pm 1SD$ is required. Common challenges in PO device design is the deterioration of accuracy due to motion artifacts, low perfusion, low saturation calibration, and probe positioning [11]. In addition to these challenges, PO with pixel arrays (hereafter referred to as camera oximetry) comes with additional design challenges. The manufacturers of consumer electronics have sole control on the choice of components for their devices. These fixed hardware options and the wide variability between devices make it more difficult for engineers to provide a generic camera oximeter solution. This manuscript aims to provide a critical analysis of technical limitations of consumer grade mobile cameras that impact PO measurements, and offers possible strategies to overcome these challenges.

II. Background

A. Pulse Oximeters

The underlying principle of PO is the Beer-Lambert law which stipulates that light intensity I_0 diminishes exponentially when traveling in an absorbing medium as follows:

$$I = I_0 e^{-\sum_{i=1}^{n} \epsilon_i(\lambda) c_i d_i}, \quad (1)$$

where ϵ_i is the extinction coefficient at a specific wavelength λ, d_i the optical path length, and c_i the concentration of substance i, and I the transmitted light intensity, under the assumption that all n substances are non-scattering and light-absorbing [11]. Oxygenated (O_2Hb) and de-oxygenated (Hb) hemoglobin have different extinction coefficients for different wavelengths (Fig. 1) and are the most important light absorbers in blood [11]. In some wavelength ranges, Hb is more absorbent than O_2Hb; in others, the absorption property is inverted. These regions are separated by isosbestic points (Fig. 1). With each pulse, the volume of blood in the

This work was supported by the Swiss National Science Foundation (SNSF) and Grand Challenges Canada (GCC).

[1]Department of Mechanical and Mechatronics Engineering, University of Stellenbosch, 7600, South Africa.

[2]Electrical & Computer Engineering in Medicine Group, Departments of Electrical & Computer Engineering and Anesthesiology, Pharmacology & Therapeutics, The University of British Columbia (UBC), 2332 Main Mall, Vancouver, BC, V6T 1Z4, Canada; contact: walter.karlen@ieee.org

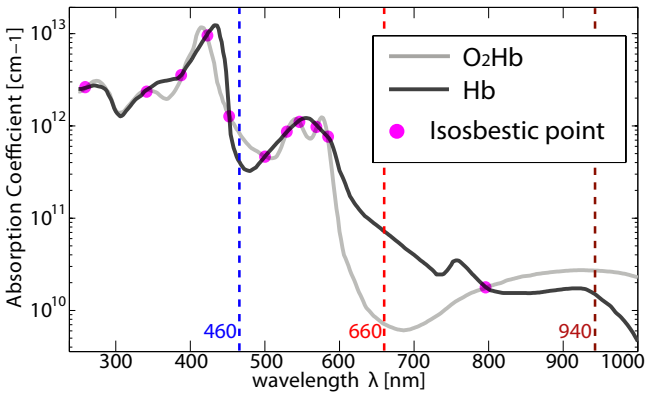

Fig. 1. Absorption curves for O_2Hb and Hb over the full visible and near IR spectrum. Circles mark isosbestic points where absorption properties for both mediums are equal. Created with data from [15].

vessels and the optical path length increase, and therefore, the total absorbance $A_\lambda = log_{10}(I_0/I)$:

$$A_\lambda = \epsilon_{O_2Hb}(\lambda)c_{O_2Hb}d_{O_2Hb} + \epsilon_{Hb}(\lambda)c_{Hb}d_{Hb}. \quad (2)$$

As a result, the variation of blood volume can be registered as a variation of transmitted light intensity and recorded with a photodetector. This produces the PPG waveform. The difference in total absorbance at two distinct wavelengths $\lambda 1$ and $\lambda 2$ allows the calculation of a modulation ratio R:

$$R = \frac{A_{\lambda 1}}{A_{\lambda 2}} = \frac{AC_{\lambda 1}/DC_{\lambda 1}}{AC_{\lambda 2}/DC_{\lambda 2}}, \quad (3)$$

where AC is the pulsatile component (from arterial blood) and DC the constant component (from venous blood, tissue, bones, etc.) of the measured PPG signal for the respective wavelengths $\lambda 1$ and $\lambda 2$ [11]. Using (3), the theoretical calibration curve for the calculation of functional oxygen saturation (SaO_2) can be described as:

$$SaO_2 = \quad (4)$$
$$\frac{\epsilon_{Hb}(\lambda 1) - \epsilon_{Hb}(\lambda 2) \times R}{\epsilon_{Hb}(\lambda 1) - \epsilon_{O_2Hb}(\lambda 1) + (\epsilon_{O_2Hb}(\lambda 2) - \epsilon_{Hb}(\lambda 2)) \times R} \times 100.$$

The Beer-Lambert law ignores scattering of light [12] and various other design aspects of individual oximeters (e.g. photodetector quantum efficiency, probe type) are not taken into account in the theoretical equation (4). To account for these effects, the relationship between R and SpO_2 is empirically determined. Even with empirical calibration, SpO_2 remains only an estimate of SaO_2.

Commercial clinical pulse oximeters use two LEDs at wavelengths in the red (e.g. 660 nm) and IR (e.g. 910 nm) spectrum to alternately illuminate the patients tissue. A photodetector measures the non-absorbed light. The illumination pattern and intensity of the LEDs is managed by a microcontroller that performs the A/D conversion and signal separation of the photodetector signal.

B. Camera Sensors

Camera sensors in modern consumer electronic devices such as mobile phones or webcams are mostly based on low-cost, power efficient and highly integrated complementary

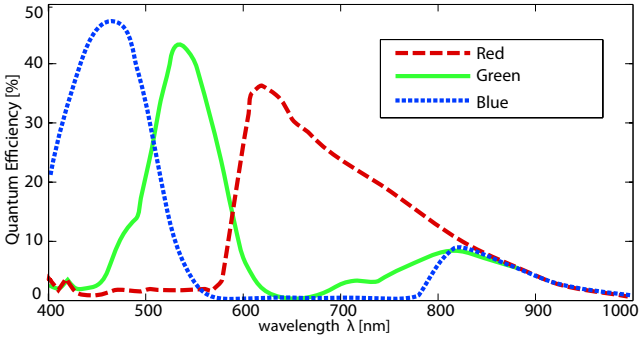

Fig. 2. Quantum efficiency for colored pixels of a high-end RGB CMOS camera sensor. Adapted from pco1600 datasheet (PCO AG, Kelheim, D).

metal-oxide-semiconductor (CMOS) technology. The sensor is an active pixel array with each pixel consisting of a photodiode and and amplifier circuit. Smartphone cameras offer resolutions of up to 41 Mpixel (808 PureView, Nokia, Finnland), but the majority of current cameras are between 2 and 8 Mpixel. Video recording is possible with resolutions of up to HD 1080p quality. The frame rate is usually limited in software to 30 fps, although 60 fps and 120 fps are possible for lower resolutions. Color images are obtained by interpolating red, green and blue (RGB) pixels in a single image. The color sensitivity of pixels is obtained by placing color filters in front of each light-active pixel. The filters are arranged in a mosaic and the most common pattern is the Bayer filter which places one red, one blue, and two green filters in a 2x2 matrix to replicate the color sensitivity of the human eye. The color sensitivity results from the transmittance of the filters and the substrate quantum efficiency (QE) (Fig. 2). The QE is not zero in the near IR range. To reduce IR glare in images taken by consumer cameras, an IR notch filter is added to the optics. CMOS sensors without an IR filter have been successfully used for PO designs [6], [7].

III. Discussion

A. Spectral Considerations

The accuracy of pulse oximeters depends largely on the stability of the spectral emission pattern of the LEDs used [16]. A shift in the emission pattern of a LED will cause an inaccuracy in the calibration curve. This is especially the case for the red LED (660 nm), which operates in a region where the absorption pattern of Hb and HbO_2 is very steep (Fig. 1) and a small shift has a large impact. To illustrate this, we have plotted the theoretical relationship between R and SaO_2 (4) for two standard wavelengths (660 nm and 940 nm) and a 10 nm shift for either the red (670 nm) or IR (950 nm) peak emission wavelength (Fig. 3). At a measured ratio $R = 1$, the expected SaO_2 is 74%. However, with a shift in the red, the expected SaO_2 is 69%, and 75% with a shift in the IR. These shifts typically occur because of manufacturing differences, variation in LED forward current, or a temperature change of the LED junction temperature during operation. A shift can vary up to $\pm$ 15 nm [16].

The use of the standard red and IR LEDs for the illumination on a consumer camera is not possible without

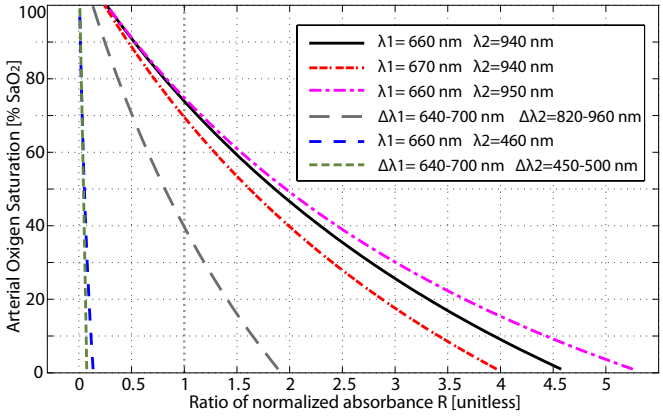

Fig. 3. Theoretical relationship between R and SaO_2 calculated for different wavelengths using (4).

modification of the camera hardware. The optical IR notch filter that blocks a considerable amount of the IR (90%) combined with the lower QE of CMOS in the IR range (Fig. 2) create a low signal-to-noise ratio. In many consumer devices it is possible to remove the notch filter. This requires dismantling the device, which is often not trivial, and will most likely void the manufacturer's warranty.

Other LED wavelengths that are not attenuated by the IR notch filter could be used. The Hb-O_2Hb absorption curve has multiple isosbestic points and therefore offers several possible ranges (Fig. 1). Three or more wavelengths in the visible spectrum are used for oximetry of retinal vessels. For example, the hyperspectral fundus camera allows imaging between 400 and 700 nm in 2 nm steps [17]. However, the absorption is much higher in the green and blue spectrum (Fig. 1). When replacing the IR LED with a blue LED (460 nm), the theoretical relationship between R and SaO_2 becomes less sensitive (Fig. 3). A change of 5% in SaO_2 corresponds to a ratio change of only 0.003. In a similar approach, the RGB filters of the CMOS sensor have been used to record a blue and red PPG [5]. Unfortunately, the blue filter of the CMOS allows a wide range of wavelengths to pass. If photons are captured over this entire range that covers 3 isosbestic points (Fig. 1), the change in ratio R related to the blue component would cancel itself out and make the measurement ambiguous. In [5], the finger was illuminated with a white phosphor based LED that has a narrow emission peak around 465 nm which might have made the observation of a correlation between R and the change in SpO_2 possible to detect. Along with using a LED with a narrow emission spectrum, narrow band-pass optical filters could be added to enhance sensitivity [18]. These solutions cannot account for the broad emission spectra of the light sources. The theoretical model (4) assumes a single peak emission wavelength for each light source. To consider a broader range of emitted light, we replaced the ϵ terms with their integral over a plausible bandwidth (red: 640-700 nm; IR: 820-960 nm; blue: 450-500 nm). This is only possible under the assumption that the emitted intensity is constant over the full bandwidth. As expected, the calibration curve

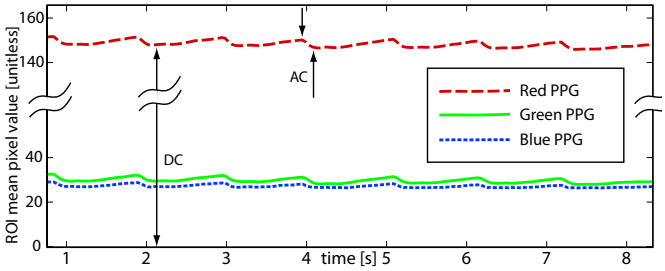

Fig. 4. RGB PPG from a mobile phone video using a region of interest (ROI) of 100^2 pixels.

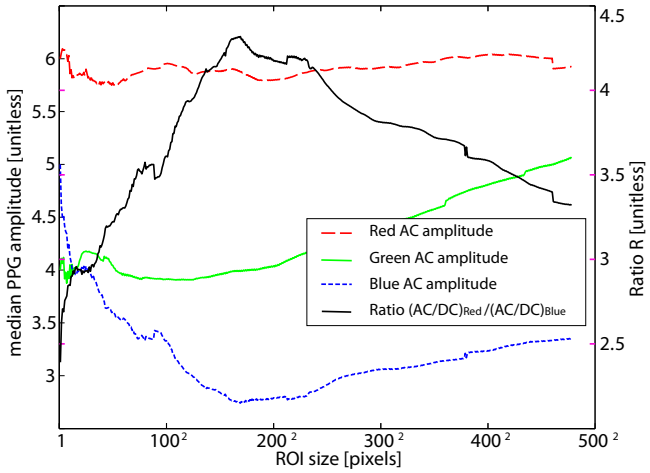

Fig. 5. RGB PPG amplitudes for different region of interest (ROI) sizes.

became less sensitive (shift to the left) for both emission pairs (Fig. 3). For a more accurate model, color filter extinction coefficients and photo detector QE must be included in (4).

B. Sensor Area

CMOS sensors offer a very high pixel count. However, the full sensor surface is not necessary for PO function. An overly large region of interest (ROI) will not produce very accurate readings and the selection of the ROI can cause difficulties with calibration [8]. To illustrate this we recorded 2 min of camera oximetry using a low cost smartphone camera (Samsung Galaxy ACE, LSI S5K4E, 5 Mpixel, auto whitebalance, contrast +2, saturation -2, VGA (640x480 pixels), 24 fps). The finger was continuously illuminated using the integrated LED flash. SpO_2 was measured using an Xpod pulse oximeter (Nonin Medical, Plymouth, USA) and was between 97% - 100% for the entire recording. The video was post-processed in Matlab (Mathworks, Natick, USA). RGB channels were separated and a RGB PPG was produced by calculating the mean of a square ROI centered on the sensor (Fig. 4). The ROI surface was varied from 1 pixel to 480^2 pixels. The AC amplitude of the PPG was extracted. While the median amplitude of the red PPG remained almost constant ($5.91 \pm 0.079SD$) over the ROI range, the amplitude of the blue PPG was reduced from 5 (1 pixel) to 2.7 (170^2 pixels). Consequently, the ratio R varied with ROI size while the SpO_2 remained constant (Fig. 5). This non-homogeneous distribution of light over the sensor

can be explained in two ways: 1) The finger on the lens is not placed in the focal plane and the resulting image is out of focus. Therefore, photons from a single point on the finger hit the sensor at multiple points. The finger is placed anterior to the focal plane and the likelihood of hitting the center is higher. 2) The image contains regions where photons have not traveled through similar path lengths and tissues. Low-wavelength photons (blue and green) have much higher skin absorbance, and therefore shorter path lengths. Only a few photons will be absorbed in the case of optical shunt (see section III-D).

C. CMOS Sensitivity

The dynamic range of standard CMOS sensors is limited to only 8-bits per color channel, resulting in 24-bits per pixel. High dynamic range (HDR) imaging sensors exist, but these are reserved for expensive cameras. Color sensitivity is described by the Bayer mosaic pattern overlaying the sensor. As there are 2 green pixels for each red and blue pixel, a higher sensitivity in the green range would be expected. Other research groups have found that green light offers a better signal-to-noise ratio when used in reflection mode with no direct illumination [8]. Although this was also suggested for transmission mode [5], we were not able to confirm this with our experiment. Independent of ROI size, the median pulse amplitude was significantly larger for red than it was for green and blue (Fig. 4). Below 600 nm, photons have a considerably lower tissue penetration depth and greater absorption in blood (Fig. 1), therefore fewer low-wavelength photons will reach the photodetector. Further experiments are required to investigate the influence of white balance algorithms and RGB demosaicing.

D. Optical Shunt

Compared to single pixel photodiodes used in conventional pulse oximeter probes, cameras have a larger field of view. This increases the risk that the sensor detects photons that did not travel through oxygenated blood (optical shunt). The effects of changing the ROI illustrated in Fig. 5 may be a result of this phenomena. Optical shunt is also possible if the finger does not completely cover the lens and ambient light reaches the sensor. The placement of the finger is therefore critical and methods to verify finger placement will need to be developed.

E. Sampling Rate

Calculation of HR and SpO_2 from the PPG requires a sampling rate of at least 25 Hz. In conventional PO the effective A/D conversion must be at least 3 times greater than the LED illumination frequency (which is greater than 450 Hz) [16]. Multiple wavelengths can be recorded simultaneously with the camera, and consequently the video frame rate can be used as the sampling rate. Under sufficient illumination, consumer grade cameras can record at a frame rate of up to 120 fps if the throughput is reduced by lowering the resolution to VGA (OV2710, OmniVision, Santa Clara, USA). This is a very interesting feature for more advanced processing, such as heart rate variability, where sampling rates as low as 100 Hz can be used [19].

IV. Conclusion

Various research groups have shown that camera oximetry with CMOS pixel arrays is possible. The technical challenges may be overcome with careful platform selection and proper understanding of the underlying mechanisms. We are currently evaluating different approaches using low-cost off-the-shelf components on subjects with low SpO_2.

References

[1] W. Karlen, G. Dumont, C. Petersen, J. Gow, J. Lim, J. Sleiman, and J. M. Ansermino, "Human-centered Phone Oximeter Interface Design for the Operating Room," in *HEALTHINF 2011 - Proceedings of the Int. Conf. on Health Informatics*, V. Traver, A. Fred, J. Filipe, and H. Gamboa, Eds. Rome, Italy: SciTePress, 2011, pp. 433–8.

[2] C. Petersen, J. M. Ansermino, and G. Dumont, "Audio phone oximeter," in *Proc. of the 2012 Society for Technology in Anesthesia Annual Meeting*. Society for Technology in Anesthesia, 2012, p. 18.

[3] M. J. Gregoski, M. Mueller, A. Vertegel, A. Shaporev, B. B. Jackson, and Others, "Development and validation of a smartphone heart rate acquisition application for health promotion and wellness telehealth applications." *Int J Telemed Appl.*, vol. 2012, pp. 1–7, 2012.

[4] E. Jonathan and M. Leahy, "Investigating a smartphone imaging unit for photoplethysmography." *Physiol Meas*, vol. 31, no. 11, pp. N79–83, 2010.

[5] C. G. Scully, J. Lee, J. Meyer, A. M. Gorbach, D. Granquist-Fraser, Y. Mendelson, and K. H. Chon, "Physiological parameter monitoring from optical recordings with a mobile phone." *IEEE Trans Biomed Eng*, vol. 59, no. 2, pp. 303–6, 2012.

[6] K. Humphreys, T. Ward, and C. Markham, "A CMOS Camera-Based Pulse Oximetry Imaging System." *Annual Int. Conf. of the IEEE Engineering in Medicine and Biology Society.* vol. 4, 3494–7, 2005.

[7] F. P. Wieringa, F. Mastik, and A. F. van der Steen, "Contactless multiple wavelength photoplethysmographic imaging: a first step toward "SpO2 camera" technology." *Ann Biomed Eng*, vol. 33, no. 8, pp. 1034–41, 2005.

[8] W. Verkruysse and L. Svaasand, "Remote plethysmographic imaging using ambient light," *Opt Express*, vol. 16, pp. 21 434–45, 2008.

[9] M.-Z. Poh, D. J. McDuff, and R. W. Picard, "Advancements in noncontact, multiparameter physiological measurements using a webcam." *IEEE Trans Biomed Eng*, vol. 58, no. 1, pp. 7–11, 2011.

[10] "ISO 80601-2-61 Medical electrical equipment Part 2-61: Particular requirements for basic safety and essential performance of pulse oximeter equipment," Geneva: International Standards Organisation, 2011.

[11] J. Webster, *Design of pulse oximeters*. NY: Taylor & Francis, 1997.

[12] P. D. Mannheimer, "The light-tissue interaction of pulse oximetry." *Anesth Analg*, vol. 105, no. 6 Suppl, pp. S10–7, 2007.

[13] Y. Mendelson and J. C. Kent, "Variations in optical absorption spectra of adult and fetal hemoglobins and its effect on pulse oximetry." *IEEE Trans Biomed Eng*, vol. 36, no. 8, pp. 844–8, 1989.

[14] I. Fine and A. Weinreb, "Multiple scattering effect in transmission pulse oximetry." *Med Biol Eng Comput*, vol. 33, no. 5, 709–12, 1995.

[15] S. Prahl, "Tabulated Molar Extinction Coefficient for Hemoglobin in Water," Oregon Medical Laser Center, Portland, Tech. Rep., 1998.

[16] J. A. Pologe, "Pulse oximetry: technical aspects of machine design." *Int Anesthesiol Clin*, vol. 25, no. 3, pp. 137–53, 1987.

[17] D. Mordant, I. Al-Abboud, G. Muyo, A. Gorman, A. Sallam, P. Rodmell, J. Crowe, and Others, "Validation of Human Whole Blood Oximetry, Using a Hyperspectral Fundus Camera with a Model Eye," *Invest Ophthalmol Vis Sci*, vol. 52, no. 5, pp. 2851–9, 2011.

[18] S. Duun, R. Haahr, K. Birkelund, P. Raahauge, P. Petersen, H. Dam, L. Noergaard, and E. Thomsen, "A Novel Ring Shaped Photodiode for Reflectance Pulse Oximetry in Wireless Applications," in *Sensors*. IEEE, 2007, pp. 596–9.

[19] P. J. Chellakumar, A. Brumfield, K. Kunderu, and W. Schopper, "Heart rate variability: comparison among devices with different temporal resolutions," *Physiol Meas*, vol. 26, no. 6, pp. 979-86, 2005.